Progress In Electromagnetics Research Letters, Vol. 99, 25–33, 2021

Printed MIMO/Diversity Antenna with Polarization Diversity

Bharghava Punna* **and Pachiyaannan Muthusamy**

Abstract—In this work, a diversity antenna with a high level of isolation is presented in this paper. To make the antenna compact, the radiating parts are arranged on opposing sides of the substrate. The isolation between the ports is sufficient for the use of a MIMO system, which is achieved through the orthogonal positioning of radiating elements. Wideband and narrowband antennas are placed on opposite sides of the substrate. The suggested monopole antenna has an impedance bandwidth of 3.1 GHz to 14.9 GHz, whereas the rectangular narrowband antenna has an impedance bandwidth of 5.4 GHz to 5.62 GHz. More than 16 dB of isolation exists between the two ports. The proposed antenna has a maximum gain of 2.9 dB. The diversity nature of the proposed MIMO antenna is studied in terms of Envelope Correlation Coefficient (ECC), Diversity Gain (DG), and Total Active Reflection Coefficient (TARC).

1. INTRODUCTION

The high data rates and high channel capacity are required for advanced communication. This can be achieved by system technology. multiple-input multiple-output (MIMO) system involves several antennas at transmitter level and receiver level for increasing data rate and capacity channel capacity without increasing spectral bandwidth or transmitted power level. The reduction in mutual coupling is achieved by placing radiators on opposite sides of the substrate as in [1]. In MIMO systems, isolation between radiators can be achieved by using L-shaped strips in the ground plane as in [2]. The reduction in the mutual coupling is accomplished by providing F-shaped stubs attached to the ground plane as represented in [3]. By the establishment of radiators orthogonal to each other, the mutual coupling is reduced in [4]. Mutual coupling is reduced in [4] by establishing radiators that are orthogonal to each other. The MIMO antenna consists of two planar-monopole (PM) radiating elements with microstrip-feeding lines printed perpendicular to each other on one side of the substrate for good isolation. Two long protruding ground stubs are added to the ground plane on the other side to improve isolation and boost impedance bandwidth, and a short ground strip is utilized to connect the ground planes of the two PMs to form a common ground [5]. To achieve good isolation, the antenna comprises two identical monopoles printed on a low-loss substrate with 3 mm spacing and positioned perpendicular to each other [6]. The two monopoles are spaced apart by a small ground portion, which serves as a layout area for the antenna feeding network, and it was found that by removing only 1.5 mm long inwards from the top edge in the small ground portion and connecting the two antennas therein with a thin printed line, the antenna port isolation can be effectively improved [7]. By including parasitic parts, a double-coupling channel is created, which can lessen mutual coupling by creating a reverse coupling. For mobile terminals, a dual-slot-element antenna with parasitic monopoles is described [8]. For MIMO applications, meandering monopoles are employed in [9], and isolation is achieved by employing a slot in the ground. An ultra-wideband (UWB) MIMO antenna for wireless device applications that covers

Received 19 May 2021, Accepted 6 July 2021, Scheduled 16 July 2021

* Corresponding author: Bharghava Punna (punnabharghava@gmail.com).

The authors are with the Advanced RF Microwave & Wireless Communication Laboratory, Vignan's Foundation for Science Technology and Research (Deemed to be University), Vadlamudi, Andhra Pradesh, India.

the WCDMA (1.92–2.17 GHz), WiMAX (2.3, 2.5 GHz), WLAN (2.4 GHz), and UWB (3.1–10.6 GHz) bands, and WLAN is rejected using an open stub is presented in [10].

The size of the MIMO antenna system is based on not only the dimensions of the individual antennas but also the technique availed to get isolation between the input ports of two individual radiators. As a result, radiators are installed on both sides of the substrate in the proposed work without the need of a decoupling network. The shapes of the radiators are different on both sides of the substrate. The novelty of the proposed work is the usage of a monopole antenna and rectangular microstrip narrowband antenna on each side of the substrate. The two radiators on both sides of the substrate are oriented orthogonally so that orthogonal feeding can be used. Two radiators' electric fields are also orthogonal. Polarization diversity is achieved because one is horizontal polarization and the other vertical polarization. To check the diversity of the presented antenna, the design methodology and results are examined.

2. DESIGN OF ANTENNA

The antenna design is depicted in Fig. 1. Radiators are considered on both sides of the substrate. The substrate used is FR4 glass epoxy with a thickness of 1.6 mm. Table 1 lists the antenna dimensions. The UWB rectangular monopole radiator is taken on an upper surface of the substrate, and its ground is in trapezium shape to get broad bandwidth. The ground considered is taken on the back side of the substrate. The design of a UWB antenna requires a lower edge frequency value, and Equation (1) represents the design step of the UWB antenna [11]

$$f_L = \frac{7.2}{L + r + P} \text{ GHz where } L, r, \text{ and } P \text{ are in cm} \tag{1}$$

In the above equation, L represents the length of the monopole radiator, r the radius of equivalent cylindrical monopole of area same as rectangular monopole radiator considered, and P the gap between the lower edge of the rectangular radiator and the upper edge of trapezium ground. A narrowband rectangular microstrip antenna is selected as the second radiator which utilizes the UWB radiator as its ground plane. This narrowband rectangular microstrip antenna is designed at WLAN frequencies 5.5 GHz. A quarter-wave transformer is utilized for impedance matching in the case of a rectangular narrowband microstrip antenna. The novelty is the usage of monopole radiator as the ground for rectangular microstrip antenna.

The proposed antenna was designed and analyzed using ANSYS HFSS version 19. The computer-generated scattering parameters are given in Fig. 2. The monopole antenna covers more than the UWB frequency range (3.1 GHz to 14.9 GHz) where WLAN frequencies are also included. The parametric

Radiator	Dimension	Value (mm)
Monopole radiator	a	22
	b	32
	c	12
	d	3
	e	17.5
	k	11
	l	10
	m	5.7
Rectangular MSA	f	3
	g	0.7
	h	14
	i	1
	j	12

Table 1. Dimensions of antenna.

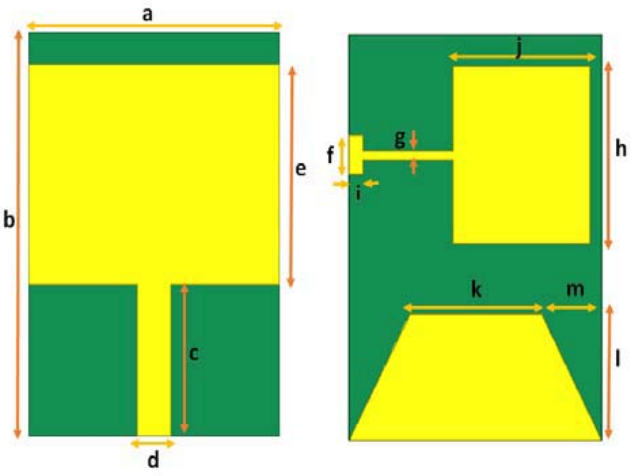

Figure 1. Proposed antenna with top orientation and bottom orientation.

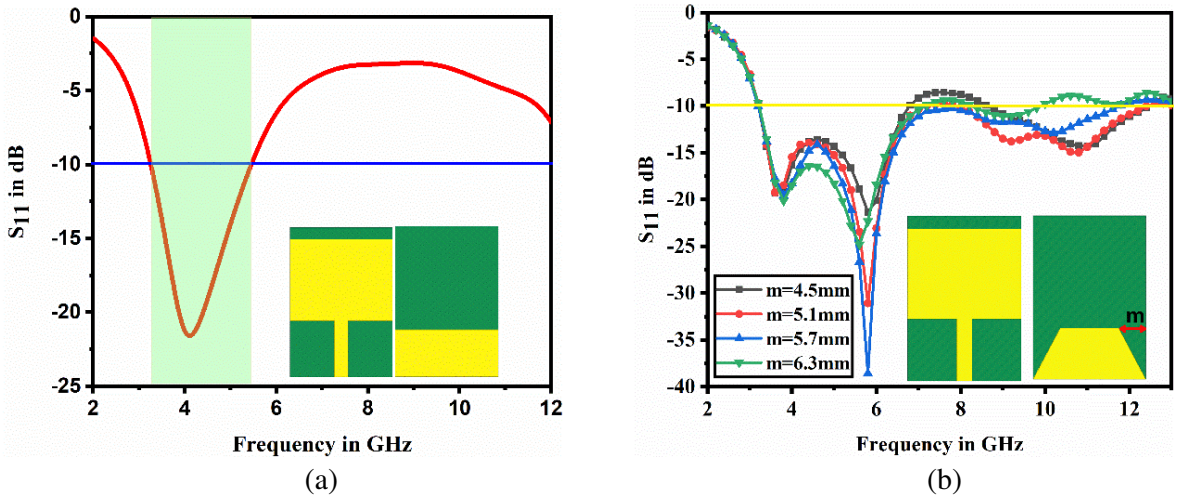

Figure 2. (a) S_{11} of monopole antenna with rectangular patch. (b) Parametric analysis of S_{11} as m changes.

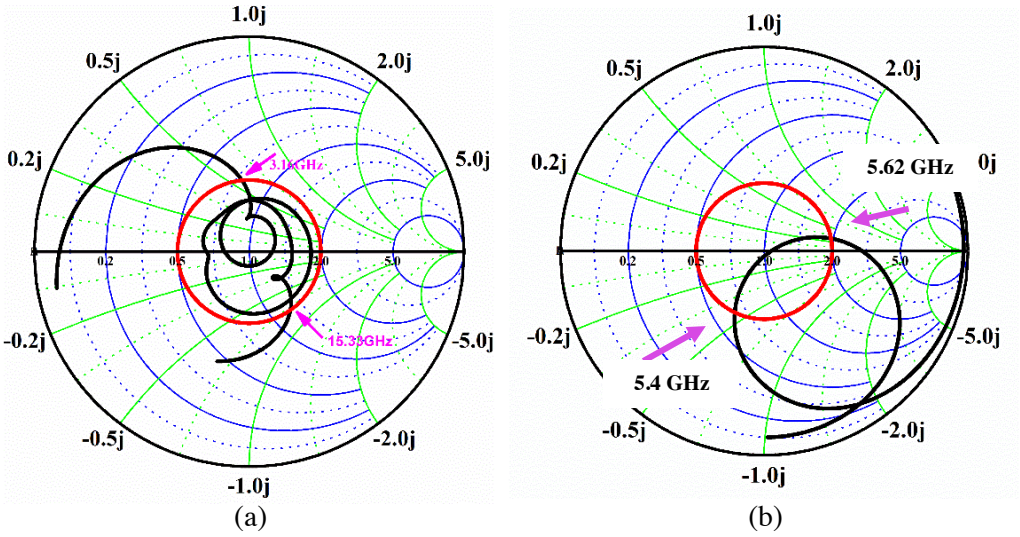

Figure 3. Smith chart impedance variations. (a) Monopole antenna. (b) rectangular microstrip antenna (RMSA).

analysis of return loss characteristics is given in Fig. 2(b), and it is understood that at trapezium shape ground parameter m of 5.7 mm, desirable impedance characteristics are obtained. The narrowband rectangular microstrip antenna covers the WLAN frequency range (5.4 GHz–5.62 GHz). The impedance characteristics of the monopole antenna and rectangular microstrip antenna can also be represented using smith chart models, which are given in Fig. 3. In Fig. 3, it is understood about impedance variations of capacitive and inductive natures of UWB monopole antenna and narrowband rectangular patch antenna when the frequency is varied. The MIMO antenna is realized by placing these radiators on two sides of a substrate where the UWB monopole patch works as a ground for a rectangular microstrip antenna. The isolation between the two ports is achieved more than 16 dB. The isolation obtained is because of the orthogonal placement of two radiators. Fig. 4 represents computer generated S-parameters of the proposed MIMO antenna. It is observed from Fig. 4 that the monopole antenna covers ultra-wideband, and rectangular microstrip patch antenna covers WLAN frequency range. The key sight vector network analyzer E5063A 100 kHz–14 GHz is used to measure the scattering parameters

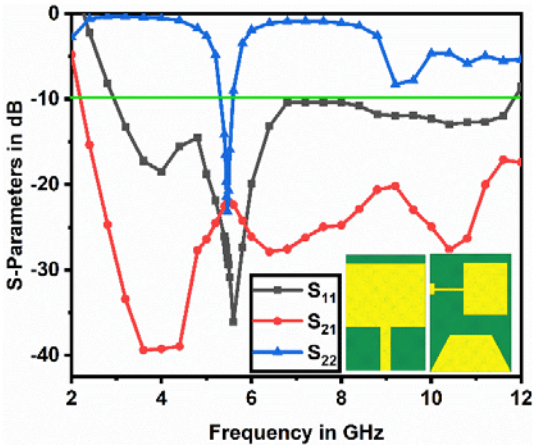

Figure 4. Simulated S-parameters.

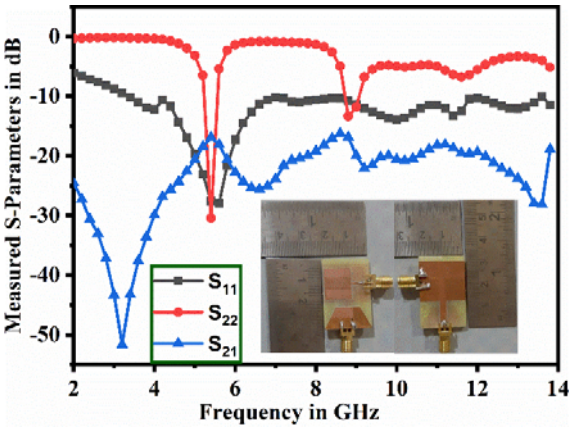

Figure 5. Measured S-parameters.

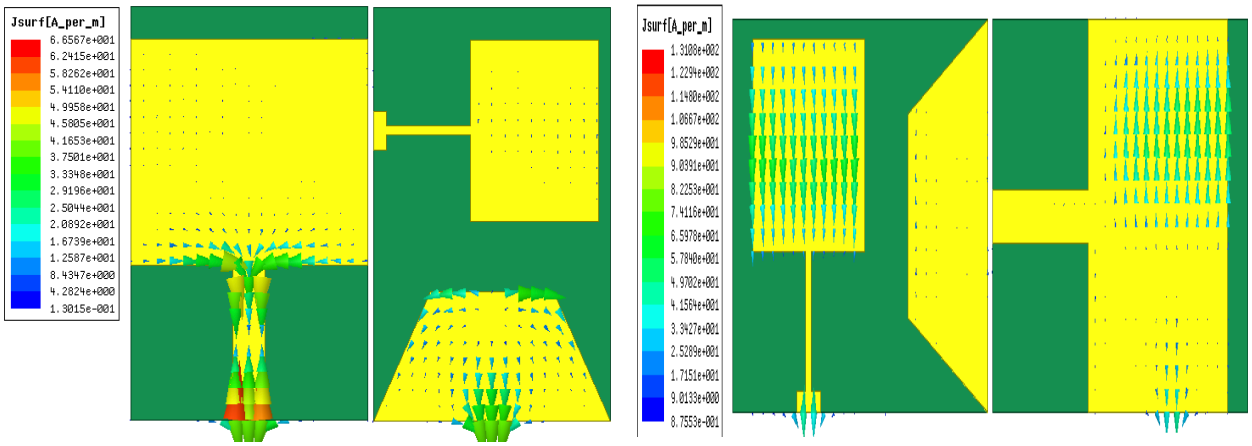

Figure 6. Current distributions (a) when port 1 is excited, (b) when port 2 is excited.

for comparing with the computer-generated scattering parameters. Fig. 5 represents measured S-parameters. The isolation between the ports is observed to be increased in the VNA measurement in comparison with computer-generated isolation values.

The surface vector current distributions on the radiating elements are responsible for the radiating nature of the antenna. It is evident from Fig. 6 that isolation is sufficient for MIMO application for the proposed MIMO antenna. From Fig. 6, no current flow in radiator 2 as long as port 1 is supplied and no current flow in radiator 1 as long as port 2 is supplied. This explains the good amount of isolation that exists between the two radiators.

3. RADIATION PATTERN ANALYSIS

Figure 7 represents a computer-generated radiation pattern in 3D view when ports are excited individually. When monopole antenna port is excited, maximum gain is 2.9 dB, and when rectangular microstrip antenna port is excited, maximum gain is 5.2 dB. These gain variations have been considered at 5.5 GHz for both radiating elements.

Figure 8 expresses the field patterns in the 2-D form at 4.8 GHz, 5.5 GHz, and 8 GHz for the proposed MIMO antenna in 2-D XZ- and 2-D YZ-planes. The suggested antenna indicates a nearly omnidirectional field pattern upon the required operational bandwidth.

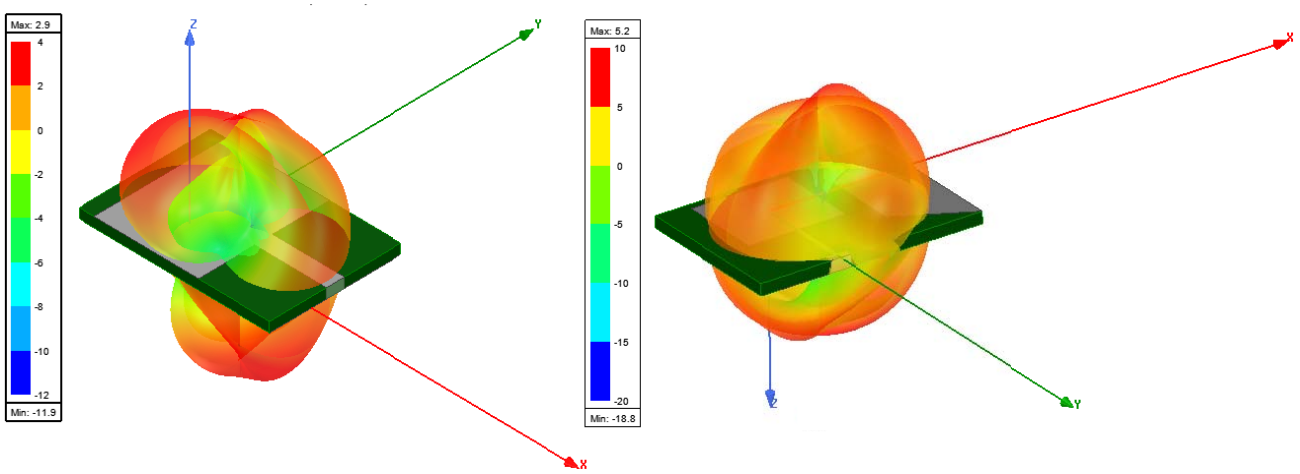

(a) (b)

Figure 7. 3D-polar plots at 5.5 GHz (a) when monopole antenna port is excited, (b) when RMSA port is excited.

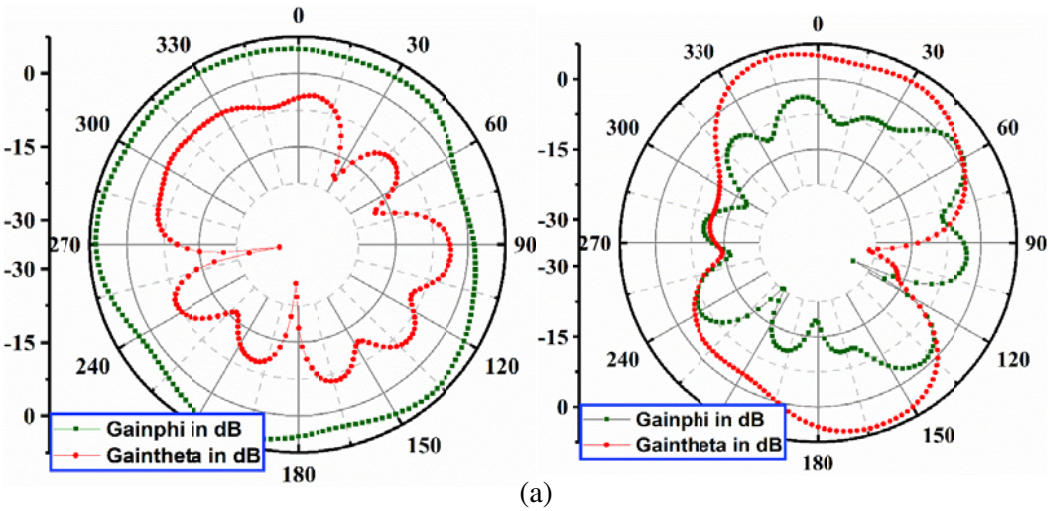

(a)

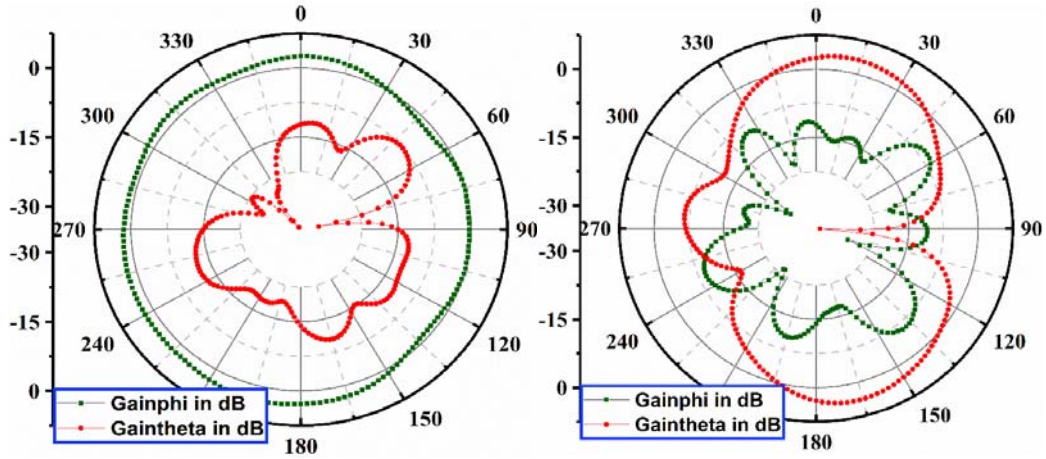

(b)

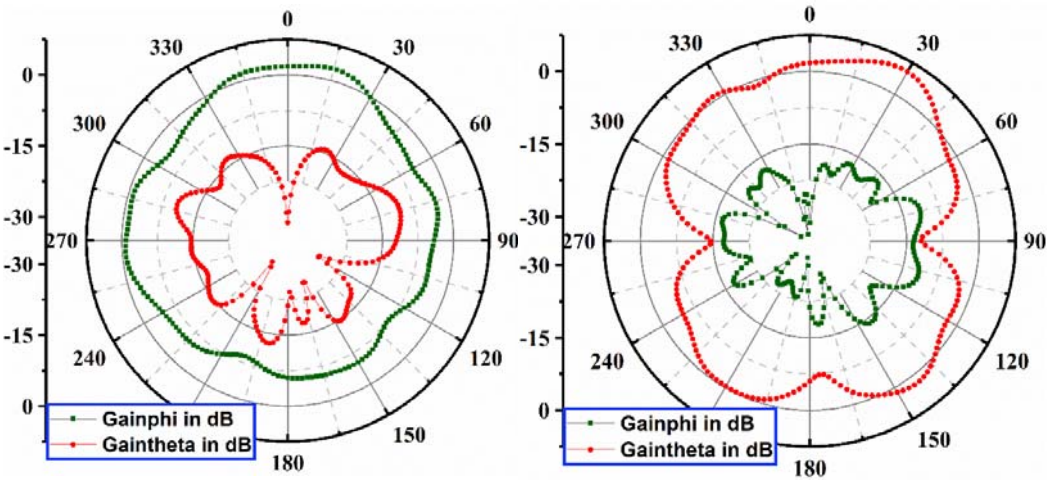

(c)

Figure 8. Gain plots (a) at 4.8 GHz, (b) at 5.7 GHz, (c) 8 GHz.

In addition, Fig. 8 represents the deterioration of radiation patterns at higher frequencies due to the splitting nature of radiation lobes. The variation in peak gain as a function frequency is shown in Fig. 9.

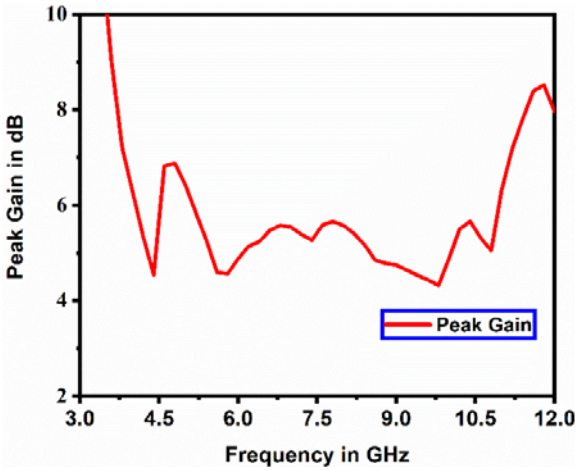

Figure 9. Peak gain of the proposed antenna with the variation in frequency.

4. DIVERSITY ANALYSIS

The diverse nature of the proposed antenna is assessed in terms of envelope correlation coefficient (ECC), diversity gain (DG), and total active reflection coefficient (TARC). The envelope correlation efficient is for the analysis of the amount of correlation between adjacent radiating elements. The envelope correlation coefficient can be computed in terms of scattering parameters.

$$\mathrm{ECC} = \frac{|S_{11}^{*}S_{12} + S_{21}^{*}S_{22}|^{2}}{(1 - S_{11}^{2} - S_{21}^{2})(1 - S_{12}^{2} - S_{22}^{2})} \tag{2}$$

The value of ECC is ideally zero in the case of a non-correlated MIMO antenna. The practical limit for ECC is < 0.5. Fig. 10 represents the computer-generated ECC plot of the suggested MIMO antenna.

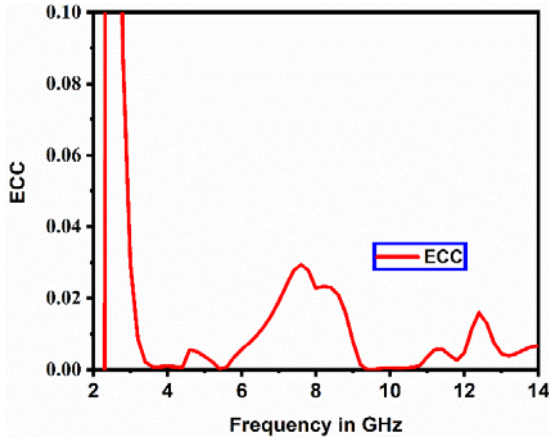

Figure 10. Envelope correlation coefficient plot.

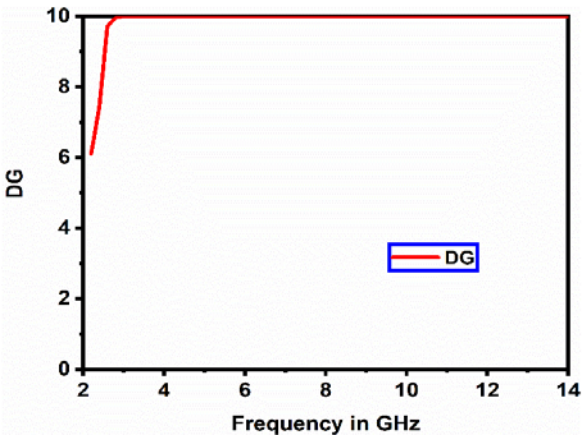

Figure 11. Diversity gain.

The value of the ECC of the suggested MIMO antenna is < 0.03 for most of the band. Another metric that can be calculated from below mentioned equation is the MIMO antenna's diversity gain

$$\mathrm{DG} = 10\sqrt{(1 - \mathrm{ECC}^2)} \tag{3}$$

Figure 11 represents diversity gain using S-parameters, and the value of diversity gain is > 9.975 dB.

The operating bandwidth and efficiency of the multiport antenna are affected due to the affecting nature of adjacent radiating elements in the multiport antenna system when they operate simultaneously, so that actual system behavior cannot be predicted using only S-parameters. The total active reflection coefficient-TARC is the metric to consider this effect. TARC is the apparent return loss of the MIMO antenna system. The parameter TARC is computed by the below-mentioned equation in the case of a 2-port MIMO system.

$$\mathrm{TARC} = \sqrt{\frac{(s_{11} + s_{12})^2 + (s_{21} + s_{22})^2}{2}} \tag{4}$$

The desirable value of TARC for the MIMO system is 0 dB. The plot for TARC of the proposed MIMO antenna is shown in Fig. 12. From Fig. 12, it is understood that TARC for the MIMO antenna is lower than -2 dB for the operating band of frequencies.

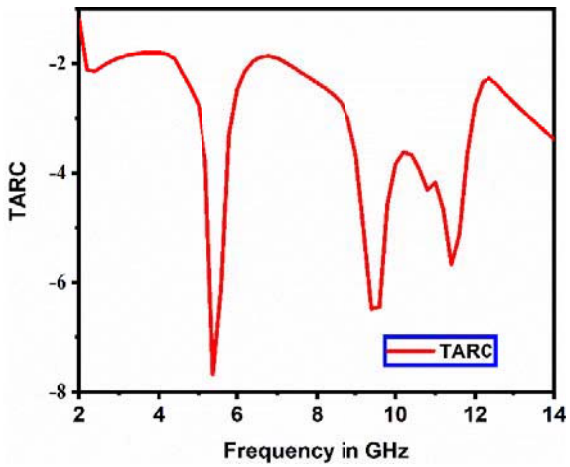

Figure 12. TARC of proposed antenna.

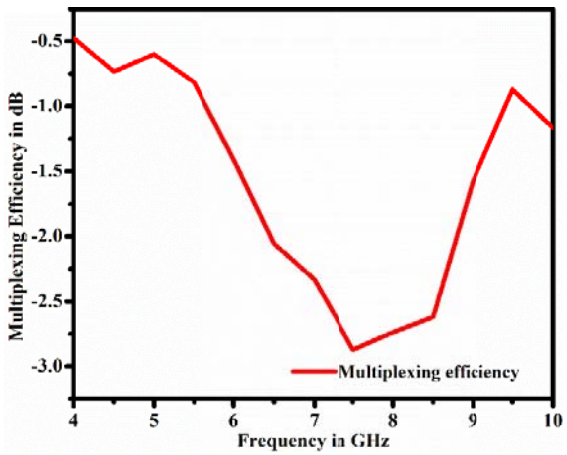

Figure 13. Multiplexing efficiency of proposed antenna.

Figure 13 shows the multiplexing efficiency with varying frequencies. Multiplexing efficiency is calculated by the following relation

$$\eta_{\text{mux}} = \sqrt{(\eta_1\eta_2)\left(1 - |\rho_c|^2\right)} \tag{5}$$

where ρ_c is the complex correlation coefficient between the radiating elements, ECC $\approx |\rho_C|^2$, and η_i is the total efficiency of the ith antenna radiator.

The fabricated proposed antenna is represented in Fig. 14. The comparison of various antennas with proposed antenna is shown in Table 2.

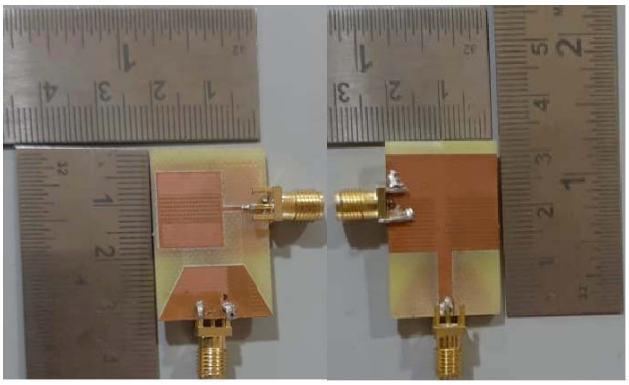

Figure 14. Fabricated antenna with top view and bottom view.

Table 2. Comparison of various antennas.

Ref	Size (mm × mm)	S_{11} in dB	Isolation in dB	Gain in dB	ECC
[1]	30 × 25	(5.5–6) and (5–6.8)	< -13	-	< 0.06
[3]	50 × 30	2.5–14.5	< -20	4.3	< 0.04
[4]	32 × 32	2.9–12	< -15	4.2	< 0.04
[5]	40 × 26	2.9–12	< -15	6.5	< 0.2
[6]	27 × 52	3.5–11.5	< -22	-	< 0.006
[7]	30 × 65	2.35–2.45	< -19	2.1	-
[9]	30 × 40	2.4, 3.1–10.6	< -16	-	< 0.15
Proposed antenna	22 × 32	(3.1–14.9) and (5.4–5.62)	< -15	2.9	< 0.07

5. CONCLUSION

In this study, a novel antenna with diversity in polarization has been proposed for the application of WLAN. The novelty is the usage of monopole radiator as the ground for a rectangular microstrip antenna. The impedance bandwidth of the proposed monopole antenna is from 3.1 GHz to 14.9 GHz, and the narrowband antenna is from 5.4 GHz to 5.62 GHz. A sufficient amount of isolation is obtained because of orthogonal placement, and even the radiators are kept on opposite faces of the substrate. The isolation between the two ports is more than 16 dB. The max gain of the proposed antenna is 2.9 dB. The polarization diversity is ensured because of different linear polarizations due to radiators. The outcomes obtained from the diversity performance specify that the proposed antenna is decent enough for MIMO applications.

ACKNOWLEDGMENT

We would like to acknowledge the Ansys software company and VFSTR (deem to be university), which has provided the Centre of Excellence (Keysight-Vignan's Advanced RF Microwave and Wireless Communications) resources. This project involved the HFSS Software extensively for the getting of simulations.

REFERENCES

1. Malik, J., A. Patnaik, and M. V. Kartikeyan, "Novel printed MIMO antenna with pattern and polarization diversity," *IEEE Antennas Wirel. Propag. Lett.*, Vol. 14, 739–742, 2015, doi: 10.1109/LAWP.2014.2377784.
2. Chandel, R., A. K. Gautam, and K. Rambabu, "Tapered fed compact UWB MIMO-diversity antenna with dual band-notched characteristics," *IEEE Trans. Antennas Propag.*, Vol. 66, No. 4, 1677–1684, Apr. 2018, doi: 10.1109/TAP.2018.2803134.
3. Iqbal, A., O. A. Saraereh, A. W. Ahmad, and S. Bashir, "Mutual coupling reduction using F-shaped stubs in UWB-MIMO antenna," *IEEE Access*, Vol. 6, 2755–2759, 2018, doi: 10.1109/ACCESS.2017.2785232.
4. Ren, J., W. Hu, Y. Yin, and R. Fan, "Compact printed MIMO antenna for UWB applications," *IEEE Antennas Wirel. Propag. Lett.*, Vol. 13, 1517–1520, 2014, doi: 10.1109/LAWP.2014.2343454.
5. Liu, L., S. W. Cheung, and T. I. Yuk, "Compact MIMO antenna for portable devices in UWB applications," *IEEE Trans. Antennas Propag.*, Vol. 61, No. 8, 4257–4264, Aug. 2013, doi: 10.1109/TAP.2013.2263277.
6. Koohestani, M., A. A. Moreira, and A. K. Skrivervik, "A novel compact CPW-fed polarization diversity ultrawideband antenna," *IEEE Antennas Wirel. Propag. Lett.*, Vol. 13, 563–566, 2014, doi: 10.1109/LAWP.2014.2312730.
7. Su, S.-W., C.-T. Lee, and F.-S. Chang, "Printed MIMO-antenna system using neutralization-line technique for wireless USB-Dongle applications," *IEEE Trans. Antennas Propag.*, Vol. 60, No. 2, 456–463, Feb. 2012, doi: 10.1109/TAP.2011.2173450.
8. Li, Z., Z. Du, M. Takahashi, K. Saito, and K. Ito, "Reducing mutual coupling of MIMO antennas with parasitic elements for mobile terminals," *IEEE Trans. Antennas Propag.*, Vol. 60, No. 2, 473–481, Feb. 2012, doi: 10.1109/TAP.2011.2173432.
9. Deng, J.-Y., L.-X. Guo, and X.-L. Liu, "An ultrawideband MIMO antenna with a high isolation," *IEEE Antennas Wirel. Propag. Lett.*, Vol. 15, 182–185, 2016, doi: 10.1109/LAWP.2015.2437713.
10. Lee, J.-M., K.-B. Kim, H.-K. Ryu, and J.-M. Woo, "A compact ultrawideband MIMO antenna with WLAN band-rejected operation for mobile devices," *IEEE Antennas Wirel. Propag. Lett.*, Vol. 11, 990–993, 2012, doi: 10.1109/LAWP.2012.2214431.
11. Thomas, K. G. and M. Sreenivasan, "A simple ultrawideband planar rectangular printed antenna with band dispensation," *IEEE Trans. Antennas Propag.*, Vol. 58, No. 1, 27–34, Jan. 2010, doi: 10.1109/TAP.2009.2036279.